

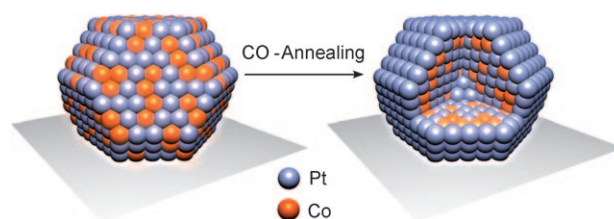
# Adsorbate-Induced Surface Segregation for Core–Shell Nanocatalysts\*\*

Karl J. J. Mayrhofer,\* Viktorija Juhart, Katrin Hartl, Marianne Hanzlik, and Matthias Arenz\*

Considering the continuously rising price of precious metals, a reduction in the amount of noble metal in catalysts is of great importance for many industrial applications. One approach is to decrease the size of catalyst particles down to the nanometer range to increase the specific surface area per mass, but also to benefit from a change in the electronic structure.<sup>[1]</sup> Core–shell catalyst structures containing an inexpensive, non-noble core surrounded by a noble-metal shell can bring about further improvements in this respect. Ideally only the catalytically active metal is located at the surface, where the reactions take place; the reaction rate should not suffer as a result of the inactive core material. A promising class of fuel-cell-cathode catalysts are alloys of platinum with other transition metals.<sup>[2–4]</sup> For these materials core–shell structures can be achieved by high-temperature annealing,<sup>[5]</sup> chemical leaching of the non-noble material,<sup>[6–8]</sup> or electrochemical deposition techniques.<sup>[9,10]</sup> All of these methods, however, exhibit significant disadvantages including the loss in active surface area and material, the formation of an incomplete noble-metal shell, and the necessity for potential control during preparation. Herein we present a novel preparation procedure of such core–shell nanoparticles with a platinum shell that overcomes these issues by using an adsorbate-induced surface segregation effect.

Depending on the heat of segregation and the surface mixing energy, the composition of the surface of a bimetallic system can be very different from the bulk.<sup>[11]</sup> This effect is additionally dependent upon the chemical potential of the gas phase, since the strong bonding of adsorbates will result in a gain in energy of the system. As a consequence, for bimetallic systems, an enrichment at the surface of the component that binds a certain adsorbate more strongly may occur.<sup>[12–14]</sup> We use this process to modify an un-leached, carbon-supported Pt<sub>3</sub>Co alloy high-surface-area catalyst (HSAC) to increase the

utilization of platinum in the particles. For this purpose the catalyst was subject to either a gas-phase treatment, or an electrochemical treatment. In the first case the catalyst powder was placed into a rotary evaporator, which was then repeatedly evacuated and filled with CO to eliminate residual oxygen. The distiller was then filled with ambient pressure of CO and heated to 200 °C for three hours. This temperature was sufficiently high to accelerate the surface segregation process without initiating the corrosion of the carbon support (see Supporting Information). For the electrochemical treatment the catalyst was placed onto a rotating disc working electrode (RDE) and subjected to a potential cycling in CO-saturated alkaline electrolyte for 60 min, so-called CO annealing.<sup>[15]</sup> Because the adsorption enthalpy of CO on Pt is higher than on Co,<sup>[16]</sup> Pt segregates to the surface of the nanoparticles, and correspondingly displaces Co to the core. Both methods lead to the same structure, comprising a Pt<sub>x</sub>Co<sub>y</sub> alloy core with a Pt shell (see Scheme 1).



**Scheme 1.** Adsorbate-induced surface segregation on bimetallic nanoparticles.

Such a surface-annealing effect can be easily detected on bulk model systems using surface-sensitive techniques, such as low-energy ion scattering.<sup>[17–19]</sup> For HSAC catalysts, however, this is generally more complicated. To determine the surface condition of the catalyst nanoparticles we used cyclic voltammetry in alkaline electrolyte (Figure 1a). By analysis of the adsorption/desorption properties in argon-purged electrolyte and comparison to an untreated Pt HSAC (Figure 1a), it is evident that the untreated catalyst surface consists of both Pt and Co atoms, whereas after CO-annealing a Pt shell containing no Co atoms has been formed on the particle surface. The broad current peaks observed at a potential of 0.7 and 0.5 V<sub>RHE</sub> (RHE = reversible hydrogen electrode), ascribed to the oxidation/reduction of Co on the surface,<sup>[20]</sup> are no longer present after the treatment with CO, so that the latter cyclic voltammogram closely resembles that of pure platinum. Moreover, for the CO-annealed catalyst, the additional oxidation peak at low potentials (0.4 V<sub>RHE</sub>) in the CO-stripping curves (Figure 1b), which is an unambig-

[\*] Dr. K. J. J. Mayrhofer, V. Juhart, K. Hartl, Dr. M. Arenz  
Lehrstuhl Physikalische Chemie, Technische Universität München  
Lichtenbergstrasse 4, 85748 Garching (Germany)  
Fax: (+49) 89-289-13389  
E-mail: karl.mayrhofer@mytum.de  
matthias.arenz@mytum.de

Dr. M. Hanzlik  
Institut für Elektronenmikroskopie  
Technische Universität München  
Lichtenbergstrasse 4, 85748 Garching (Germany)

[\*\*] This work was supported by the DFG through the Emmy-Noether project ARE852/1-1. K.M. thanks the Austrian FWF for an Erwin-Schrödinger Scholarship. We thank Dr. T. Tada from Tanaka Kikinokogyo for the supply of the catalyst.

Supporting information for this article is available on the WWW under <http://dx.doi.org/10.1002/anie.200806209>.

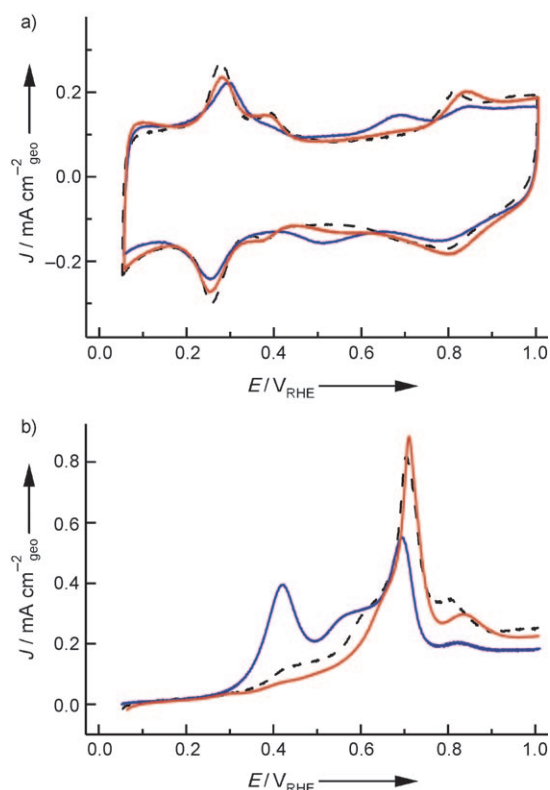


**Figure 1.** Cyclic voltammetry (a) and CO stripping (b) of CO-annealed  $\text{Pt}_3\text{Co}$  (red), untreated  $\text{Pt}_3\text{Co}$  (blue) catalysts in alkaline electrolyte purged with argon. A plain Pt HSAC catalyst is shown for comparison (black dashed).

uous sign of Co surface atoms, is not present anymore. The CO-annealed catalyst is inferior to the untreated Pt–Co alloy in oxidizing adsorbed CO because it lacks the bi-functional reaction centers; as a result it behaves like a pure Pt HSAC.

The core–shell nanoparticles were also investigated as possible catalyst candidates for oxygen reduction (ORR), which is a key reaction in fuel-cell technology. Studies on polycrystalline and single-crystal model systems have shown that alloying Pt with a first-row transition metal leads to an increase in specific activity by a factor of 2–4.<sup>[7,19]</sup> A similar improvement in catalytic activity could be observed on the CO-annealed  $\text{Pt}_3\text{Co}$  HSAC in this study (see Table 1). In alkaline solution the activity normalized to the mass of Pt of the untreated  $\text{Pt}_3\text{Co}$  catalyst is comparable to that of a Pt HSAC catalyst, whereas after a CO-annealing treatment, it increases significantly by a factor of 2.5–3. In acid electrolyte

**Table 1:** Comparison of the ORR mass activities and specific activities.<sup>[a]</sup>

ORR	Pt/5 nm	$\text{Pt}_3\text{Co}^{[b,c]}$	$\text{Pt}_3\text{Co}^{[d]}$	$\text{Pt}_3\text{Co}^{[e]}$
0.1 M KOH	0.12	0.13	0.29	0.36
0.1 M $\text{HClO}_4$	0.45	0.86	1.15	

[a] At 0.900  $V_{\text{RHE}}$  in 0.1 M KOH [ $\text{mA } \mu\text{g}_{\text{Pt}}^{-1}$ ] and 0.1 M  $\text{HClO}_4$  [ $\text{mA cm}^{-2}_{\text{real}}$ ], respectively. The estimated error of the absolute values is  $\pm 10$ –15%.

[b] Untreated catalyst (KOH). [c] Leached catalyst ( $\text{HClO}_4$ ). [d] In situ CO annealed. [e] Gas-phase CO annealed.

the CO-annealed  $\text{Pt}_3\text{Co}$  catalyst also shows superior activity; compared to plain Pt HSAC the specific activity increased by a factor of 3 (Figure 2). Interestingly, the CO-annealed  $\text{Pt}_3\text{Co}$

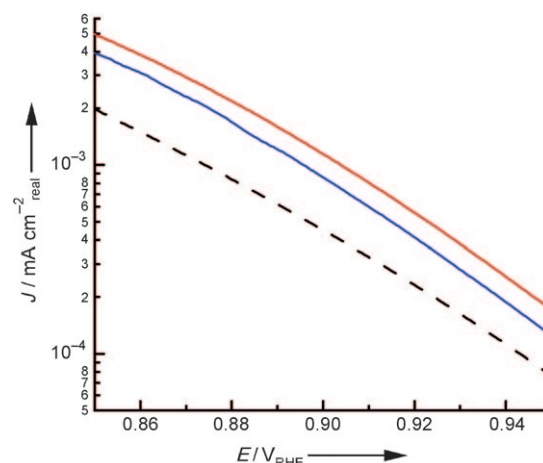


**Figure 2.** Tafel plot of ORR on CO-annealed  $\text{Pt}_3\text{Co}$  (red), chemically leached  $\text{Pt}_3\text{Co}$  (blue), and plain Pt HSAC (black dashed) catalysts. Electrolyte: 0.1 M  $\text{HClO}_4$ , room temperature, 50  $\text{mV s}^{-1}$ .

nanoparticles are also more active than the chemical-leached sample, as has recently been reported for  $\text{Pt}_3\text{Co}$  bulk alloys.<sup>[19]</sup> This result is additional confirmation that CO annealing induces a similar effect as thermal annealing, that is, forming a Pt shell around an alloy core without any leaching of Co into the electrolyte (see Supporting Information). In contrast to thermal annealing, however, CO annealing is better suited for nanocatalysts, since the particle size remains unaltered (see Supporting Information) and no active-surface-area loss occurs.

In conclusion, nanoparticles consisting of a Pt shell around a  $\text{Pt}_x\text{Co}_y$  core were formed by utilizing an adsorbate-induced surface segregation effect, resulting in a highly active catalyst with a low amount of noble metal. Such catalysts prepared by this CO annealing procedure have very promising potential, not only for the oxygen reduction, but also for other reactions requiring noble-metal surfaces.

## Experimental Section

The electrochemical measurements were conducted in a three-compartment electrochemical Teflon-cell, using a rotating disc electrode setup (Radiometer Analytical, France) and potentiostat (Bank, Germany). A saturated calomel electrode and a graphite rod were used as reference and counter electrodes, respectively. The electrolyte was prepared using Milli Q water (Millipore), KOH pellets and conc.  $\text{HClO}_4$  (both Suprapure; Merck, Germany). For experimental details regarding the catalyst-film preparation, electrochemical measurements, and further catalyst characterization see the Supporting Information.

Received: December 19, 2008

Published online: April 6, 2009

**Keywords:** core-shell nanoparticles · fuel cells · supported catalysis · oxygen reduction · surface segregation

- [1] R. Schlögl, S. B. A. Hamid, *Angew. Chem.* **2004**, *116*, 1656; *Angew. Chem. Int. Ed.* **2004**, *43*, 1628.
- [2] V. Ponec, *Appl. Catal. A* **2001**, *222*, 31.
- [3] V. R. Stamenkovic, B. Fowler, B. S. Mun, G. Wang, P. N. Ross, C. A. Lucas, N. M. Markovic, *Science* **2007**, *315*, 493.
- [4] T. Toda, H. Igarashi, M. Watanabe, *J. Electrochem. Soc.* **1998**, *145*, 4185.
- [5] S. Koh, J. Leisch, M. F. Toney, P. Strasser, *J. Phys. Chem. C* **2007**, *111*, 3744.
- [6] R. Srivastava, P. Mani, N. Hahn, P. Strasser, *Angew. Chem.* **2007**, *119*, 9146; *Angew. Chem. Int. Ed.* **2007**, *46*, 8988.
- [7] T. Toda, H. Igarashi, M. Watanabe, *J. Electroanal. Chem.* **1999**, *460*, 258.
- [8] H. Uchida, H. Ozuka, M. Watanabe, *Electrochim. Acta* **2002**, *47*, 3629.
- [9] S. Papadimitriou, A. Tegou, E. Pavlidou, S. Aramyanov, E. Valova, G. Kokkinidis, S. Sotiropoulos, *Electrochim. Acta* **2008**, *53*, 6559.
- [10] J. Zhang, F. H. B. Lima, M. H. Shao, K. Sasaki, J. X. Wang, J. Hanson, R. R. Adzic, *J. Phys. Chem. B* **2005**, *109*, 22701.
- [11] A. Christensen, A. V. Ruban, P. Stoltze, K. W. Jacobsen, H. L. Skriver, J. K. Nørskov, F. Besenbacher, *Phys. Rev. B* **1997**, *56*, 5822.
- [12] J. Nerlov, I. Chorkendorff, *Catal. Lett.* **1998**, *54*, 171.
- [13] V. Ponec, *Surf. Sci.* **1979**, *80*, 352.
- [14] Y. Yin, R. M. Rioux, C. K. Erdonmez, S. Hughes, G. A. Somorjai, A. P. Alivisatos, *Science* **2004**, *304*, 711.
- [15] M. Arenz, K. J. J. Mayrhofer, V. R. Stamenkovic, B. B. Blizanac, T. Tada, N. M. Markovic, P. N. Ross, *J. Am. Chem. Soc.* **2005**, *127*, 6819.
- [16] Y. Gauthier, M. Schmid, S. Padovani, E. Lundgren, V. Bus, G. Kresse, J. Redinger, P. Varga, *Phys. Rev. Lett.* **2001**, *87*, 036103.
- [17] U. Bardi, B. C. Beard, P. N. Ross, *J. Catal.* **1990**, *124*, 22.
- [18] K. S. Shpiro, N. S. Telegina, V. M. Gryaznov, K. M. Minachev, Y. Rudny, *Catal. Lett.* **1992**, *12*, 375.
- [19] V. R. Stamenkovic, B. S. Mun, M. Arenz, K. J. J. Mayrhofer, C. A. Lucas, G. F. Wang, P. N. Ross, N. M. Markovic, *Nat. Mater.* **2007**, *6*, 241.
- [20] M. Pourbaix, *Atlas of electrochemical equilibria in aqueous solutions*, 2nd English ed., National Association of Corrosion Engineers, Houston, **1974**.